Article

Not peer-reviewed version

Tracing Local Production and Agricultural Trade: A Multi-Analytical Study of Roman Amphorae at Conímbriga (Central Portugal)

Ida Buraca , César Oliveira , Carlo Bottaini , Vírgilio Hipólito Correia , Nicola Schiavon , José Mirão , Massimo Beltrame *

Posted Date: 27 August 2025

doi: 10.20944/preprints202508.1919.v1

Keywords: amphorae; Roman economy; ceramics production; chemical analysis

 doi:10.20944/preprints202508.1919.v1

Article

Tracing Local Production and Agricultural Trade: A Multi-Analytical Study of Roman Amphorae at Conímbriga (Central Portugal)

Ida Buraca [1,2], César Oliveira [3,4], Carlo Bottaini [3,4], Vírgilio Hipólito Correia [2,5], Nicola Schiavon [3,4], José Mirão [3,4] and Massimo Beltrame [3,4,*]

[1] Faculty of Arts and Humanities of the University of Porto, Via Panorâmica, s/n, 4150-564, Porto, Portugal
[2] Center for Classical and Humanistic Studies, CECH, Faculty of Arts and Humanities of the University of Coimbra, 5th floor, Largo da Porta Férrea, 3004-530 Coimbra, Portugal
[3] Laboratório HERCULES, Universidade de Évora, Largo dos Colegiais 2, 7004-516 Évora, Portugal
[4] Laboratório Associado In2Past, Universidade de Évora, Portugal
[5] Conimbriga National Museum, Condeixa-a-Velha, Portugal
* Correspondence: massimo@uevora.pt

Abstract

Amphorae are a significant type of Roman pottery, serving as both transport containers and indicators of economic and technological practices across the Empire. Despite their importance in interpreting local economic dynamics in Roman Lusitania, the production origins, technological characteristics and functional roles of amphorae from Conímbriga in Portugal remain poorly understood. Previous research has focused primarily on typological comparisons with imported forms, providing limited insight into whether these vessels were produced locally or how they were incorporated into regional trade and agricultural systems. This study takes a multi-analytical approach to examine a group of ten amphorae dating from the 1st to the 5th century AD. While these vessels formally resemble well-known types from Gaul and Hispania, they appear to have been manufactured locally using fabrics consistent with those found in regional common wares. To examine the raw materials, production techniques and possible contents, the analysis integrates a typological assessment with a range of archaeometric methods, including optical microscopy (OM), X-ray diffraction (XRD), X-ray fluorescence (XRF) and scanning electron microscopy with energy-dispersive spectroscopy (SEM-EDS). Recent gas chromatography–mass spectrometry (GC–MS) results contextualise these data further, enabling an exploration of how specific technological choices may have influenced or reflected the intended function of the amphorae. The findings shed new light on local ceramic production and contribute to broader debates concerning Roman provincial economies and material culture.

Keywords: amphorae; Roman economy; ceramics production; chemical analysis

1. Introduction

The Roman city of Conímbriga is located in central Portugal, within the municipality of Condeixa-a-Nova (district of Coimbra). Since 1930, it has been the focus of systematic archaeological excavations, which have brought to light one of the most significant urban centres of Roman Lusitania (Figure 1).

 doi:10.20944/preprints202508.1919.v1

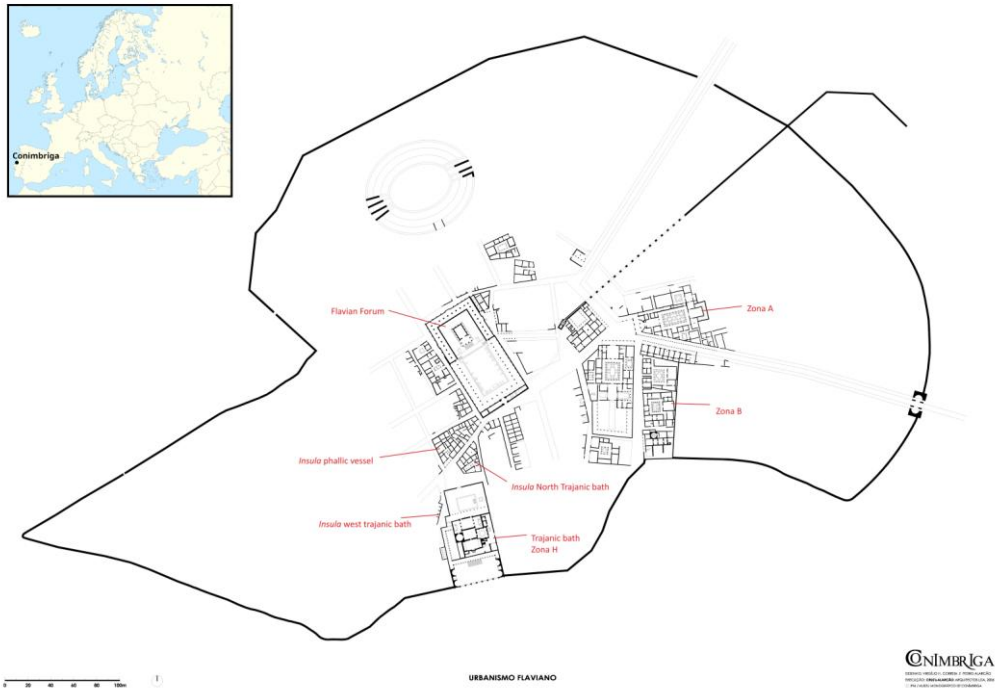

Figure 1. Plan of the Roman city of Conímbriga.

The area later occupied by Conímbriga was already settled in Late Prehistory, with archaeological evidence pointing to a Late Bronze Age occupation and the presence of an Iron Age oppidum. Following the military campaign of Decimus Junius Brutus, the region gradually came under Roman influence, and around 27 BC it was formally integrated into the newly established province of Lusitania [1].

Under Roman rule, a new city was founded and underwent substantial expansion over the following centuries. From the end of the 1st century BC, a comprehensive Augustan urban development programme was launched, including the construction of major infrastructures such as a defensive wall, an aqueduct, a road network, a Forum, and public baths. Archaeological evidence suggests that this phase of construction began around 10 BC [2].

A significant urban transformation occurred between the Flavian period and the 2nd century AD, during the reign of Emperor Vespasian. This development was likely linked to the extension of Latium Minus to the whole of Hispania and to the granting of the honorary title Flavia to the city of Conímbriga [3]. In this period, the Forum was extensively remodelled and expanded, becoming a sanctuary dedicated to the imperial cult in the final quarter of the 1st century AD. The so-called Trajanic Baths were probably constructed shortly after the Forum's renovation, in the early 2nd century AD [4].

The Late Imperial period appears to have begun with the construction of a new defensive wall that reduced the city's perimeter—an intervention generally interpreted as a response to increasing external threats. This fortification has been dated to the late 3rd or early 4th century AD [5]. Despite suffering Suevic attacks in 465 and 468 AD—which resulted in the destruction of several buildings and the capture of the wife and children of Cantaber, a prominent local figure—the city continued to be inhabited [6]. Stratigraphic evidence from substantial rubbish deposits suggests a concentration of population during this period. Between 561 and 580 AD, Conímbriga became the seat of a district under Bishop Lucentius. Radiocarbon dating of the latest occupational phases confirms continued settlement at the site until at least the 12th century AD [7].

The reconstruction of Conímbriga's long-term occupation has been made possible largely thanks to systematic archaeological investigations. A milestone in this process was the publication, in 1976, of the results of the Portuguese-French excavations conducted between 1964 and 1973, collected in

 doi:10.20944/preprints202508.1919.v1

Fouilles de Conimbriga [8]. This work marked the beginning of an intensive research programme focused on the site's ceramic assemblages. By combining typological and archaeometric approaches, it enabled the identification of locally produced orange common wares. However, due to the highly fragmented nature of the material, amphorae remained among the least thoroughly studied ceramic classes, leaving this area of research relatively underdeveloped.

Nonetheless, some ceramic finds provide indirect evidence for the exportation of agricultural goods produced on a local or regional scale. The presence of dolia—large ceramic containers typically used for the production and storage of wine and olive oil—points to agricultural activity in the area [1,9,10]. Moreover, the limited number of imported oil amphorae recovered at the site suggests a pattern of local production and a likely distribution network operating on a regional scale. Wine amphorae dated to the late 1st and early 2nd centuries AD further support the existence of regional commercial circuits for agricultural surplus.

Given that the economy of a Roman city was fundamentally rooted in agriculture, it is plausible that products such as wine, olive oil, and cereals were intended not only for local consumption but also for redistribution. Investigating the provenance of amphorae from Conímbriga therefore offers a valuable opportunity to enhance our understanding of the city's economic role within its territory and the broader dynamics of production and distribution in Roman Lusitania.

As part of a recent chrono-typological reassessment, a group of amphorae exhibiting consistent manufacturing features has been identified, despite their typological variability (10). These include Dressel 2–4, flat-bottomed forms comparable to Gauloise 4 and 5, and Dressel 28, as well as several regionally defined types provisionally designated as Conimbriga 1, Conimbriga 2, and Conimbriga 45/46. Hundreds of amphora fragments were examined macroscopically, with particular attention to ceramic fabrics and temper inclusions. From this assemblage, a representative subset of ten amphorae was selected to reflect a broad spectrum of typological and chronological variation. The primary objective was to establish a robust analytical protocol to determine whether these amphorae were locally produced, and to assess how their technological characteristics and raw materials correspond to regional ceramic traditions.

To address these questions, an integrated, multi-analytical methodology was applied. This approach combined traditional typological analysis with a suite of archaeometric techniques, including optical microscopy (OM), X-ray diffraction (XRD), X-ray fluorescence (XRF), and scanning electron microscopy coupled with energy-dispersive spectroscopy (SEM-EDS). Additionally, these archaeometric data were integrated with the results of recently published gas chromatography–mass spectrometry (GC–MS) analyses carried out on four of the amphora fragments included in the present study. This integration was aimed at exploring how specific technological choices may have influenced, or reflected, the intended function of these vessels within local and regional economic systems.

2. Materials and Methods

2.1. Materials

The archaeometric analysis focused on a total of ten amphora fragments representing a typologically diverse group of forms commonly associated with the Roman Imperial period. The sample includes one fragment of Conimbriga 1, two of Dressel 2–4, one of Dressel 28, three of Gauloise 4, one of Conimbriga 2, and two of Conimbriga 45/46 (Figure 2).

Chronologically, the assemblage spans the 1st to 5th centuries AD (Table 1). The selection was based on typological criteria, with the aim of assembling a representative sample relevant to local production and regional distribution dynamics during the Roman occupation.

 doi:10.20944/preprints202508.1919.v1

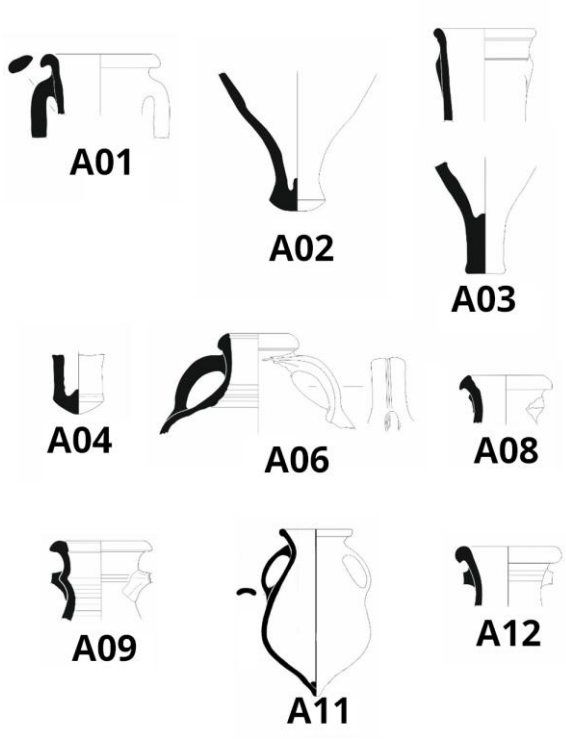

Figure 2. Drawings of a representative group of amphorae analysed in this paper.

A preliminary macroscopic examination was undertaken to identify variations in ceramic fabric, texture, and firing conditions. Based on visual and tactile assessments, the fragments were classified according to their technological attributes and differences in raw material preparation.

Most samples—specifically A01, A02, A05, A06, A08, and A12—exhibit a very hard and compact red-brown paste, consistent with firing in an oxidising atmosphere. These fabrics are notably homogeneous and contain very few non-plastic inclusions, suggesting the use of well-processed clays and a controlled production environment.

By contrast, samples A03, A09, and A10 display significantly coarser textures. Their matrices contain abundant large inclusions—both opaque and transparent—alongside small reddish particles and a notable presence of shiny, mica-like minerals. These features indicate different choices in clay selection and preparation. Sample A11 (Conimbriga 45/46 type) shares many of these characteristics but is distinguished by an even higher density of coarse inclusions and mica flakes. Such traits may point to a distinct geological source or to a separate production tradition within the broader ceramic landscape.

Table 1. Summary of the analyzed amphora fragments.

Lab ID	Archaeological ID	Type	Chronology
A01	2004_IWT_2	Conimbriga 1	1st to 3rd century AD
A02	2004_IWT_4	Dressel 2-4	1st century AD (from 69 to 96 AD)
A03	66_H_VI_44_6	Dressel 2-4	1st century AD (from 69 to 96 AD)
A05	67_H_VI_43_9	Dressel 28	Prior to the 3rd century AD
A06	66_U_11	Gauloise 4	Prior to the end of the 3rd century AD
A08	66_F_1/67/12	Gauloise 4	Prior to the end of the 3rd century AD
A09	69_H_VIII_47_5	Conimbriga 2	4th century AD to last quarter of 5th century AD (from 305 to 476 AD)
A10	72_BF6_10	Conimbriga 45-46	Last quarter of the 1st century AD to the 3rd century AD
A11	71_CRY_Norte_Cano	Conimbriga 45-46	Last quarter of the 1st century AD to the 3rd century AD
A12	72_BF1_7	Gauloise 4	Prior to the end of the 3rd century AD

 doi:10.20944/preprints202508.1919.v1

This macroscopic classification provided the foundation for the subsequent analytical investigations, which aimed to refine the technological characterisation of the fabrics and assess their implications for ceramic production strategies and regional supply systems.

2.2. Methods

To refine the preliminary macroscopic observations and gain deeper insight into the technological characteristics of the ceramic assemblage, a set of complementary analytical techniques was employed. These methods enabled the investigation of mineralogical composition, chemical signatures, and microstructural features through OM, XRD, XRF, and SEM-EDS. The integrated application of these techniques provided a robust analytical framework for reconstructing raw material selection and manufacturing processes.

2.2.1. Optical Microscopy

Petrographic analysis was conducted on thin sections using a Leica DM-2500P polarised light microscope equipped with an image acquisition system. Descriptions of the clay matrix, non-plastic inclusions (i.e. temper), and porosity follow the classification scheme proposed by Quinn [11]. Image analysis was performed using ImageJ software (version 1.54) to quantify grain size, distribution, and the relative abundance of components. Measurements were based on binary images acquired under plane-polarised light (PPL) and cross-polarised light (XPL). Grain size classification was based on the Wentworth scale [12].

2.2.2. X-Ray Diffraction

XRD analyses were carried out on powdered samples using a Bruker™ AXS D8 Discovery diffractometer (Da Vinci design), equipped with a Cu Kα radiation source (λ = 1.5406 Å), operating at 40 kV and 40 mA, and fitted with a LynxEye 1D detector. Scans were recorded over a 3°–75° 2θ range, with a step size of 0.05° 2θ and an acquisition time of 1 second per step. Mineral identification was performed using Diffract EVA 5.0 software and the PDF-2 database (ICDD). The resulting mineralogical profiles were interpreted with particular attention to high-temperature phase transformations, in order to reconstruct the thermal history of the ceramic pastes.

2.2.3. X-Ray Fluorescence

Major element concentrations were determined using a Bruker™ S2 PUMA energy-dispersive X-ray fluorescence (ED-XRF) spectrometer fitted with a silver tube. The instrument was calibrated using 36 certified reference materials. Samples were analysed as fused glass beads, prepared using a 1:10 sample-to-flux ratio. Quantitative data were processed using Spectra Elements 2.0 software. Loss on ignition (LOI) was measured by calcining approximately 1 g of powdered sample at high temperature.

2.2.4. Scanning Electron Microscopy with Energy-Dispersive Spectroscopy

Microstructural and chemical characterisation of the ceramic matrix was performed using a Hitachi™ S-3700N variable pressure SEM, equipped with a Bruker™ XFlash 5010 silicon drift EDS detector (resolution: 129 eV at FWHM/Mn Kα). Analyses were conducted at an accelerating voltage of 20 kV, beam current of 120 µA, and chamber pressure of 40 Pa. Elemental data were converted to oxides by stoichiometric calculation and normalised to 100%, based on three replicate measurements per sample. Data acquisition and interpretation were carried out using Esprit 1.9 software (Bruker).

 doi:10.20944/preprints202508.1919.v1

3. Results and Discussion

3.1. Technological Analysis and Raw Material Characterization

Petrographic observations conducted under optical microscopy revealed marked compositional and textural variability among the samples, allowing their classification into two main fabric groups (Figure 3). These differences provide insight into raw material procurement strategies, clay preparation techniques, and firing conditions. Full petrographic data are presented in Tables 2 to 4.

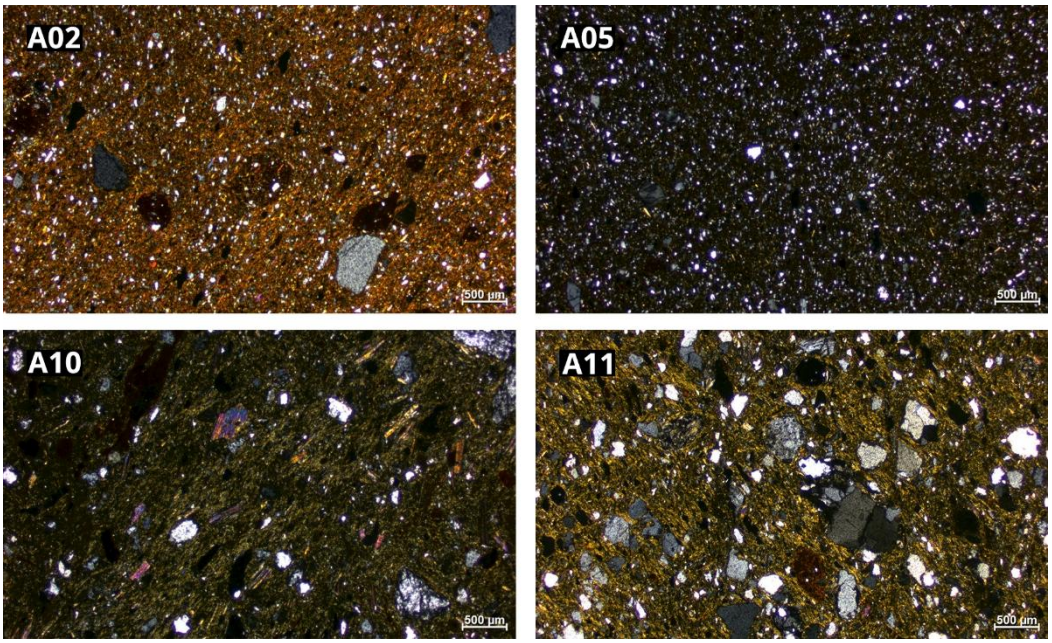

Figure 3. Photomicrographs of ceramic thin sections taken under crossed polars (XPL) at 25× magnification.

The first group comprises samples A01, A02, A03, A05, A06, and A12, which exhibit a remarkably homogeneous ceramic matrix characterised by a reddish-brown colour and pronounced optical activity under crossed polarized light. The reddish hue indicates iron oxide enrichment distributed uniformly within the ceramic body. Sample A12 is notable for its isotropic matrix, consistent with a high degree of vitrification likely linked to elevated firing temperatures. Porosity in these samples is mainly represented by vesicles and channels, ranging in size from micro- to macro-scale, reflecting a relatively closed and compact fabric.

The temper consists predominantly of rounded to sub-rounded, equidimensional grains spanning coarse silt to very coarse sand size fractions. Grain size distribution is typically unimodal, with a dominance of finer fractions, although sample A08 displays bimodal distribution. Grain roundness varies from angular to well-rounded, with rounded grains prevailing, indicative of transport and sorting processes prior to incorporation. Temper concentration reaches up to approximately 20%, with inclusions densely and evenly dispersed throughout the matrix. The temper is moderately to well sorted, with grains exhibiting moderate to strong preferred orientation in some samples.

Mineralogically, these samples contain quartz, potassium feldspar, plagioclase feldspar, muscovite, and opaque minerals as primary temper constituents, with occasional amphibole detected (notably in sample A05). Rare fragments of quartzite and granitoid lithics were also identified, albeit infrequently. The presence of isolated clay pellets embedded in the matrix suggests incomplete mixing of raw clays or intentional inclusion of specific clay types.

The technological homogeneity across this group implies a shared production tradition, most likely reflecting local ceramic workshops producing different types of amphorae. The consistent presence of small, rounded temper grains—likely intentionally added—and the overall granular

 doi:10.20944/preprints202508.1919.v1

fabric suggest that raw clays were subjected to decantation or sieving to remove coarser impurities before forming. The rounded morphology and sorting of inclusions strongly support a fluvial sedimentary origin of the raw materials, consistent with alluvial deposits.

Provenance considerations align with this interpretation, indicating exploitation of clay and temper sources within the Meso-Cenozoic sedimentary basin of the Mondego River, situated near Conímbriga. This basin comprises varied sedimentary lithologies including Quaternary to Cretaceous alluvial sands, sandstones, siltstones, conglomerates, pelites, and subordinate carbonates such as limestones and marls. The chronological distribution of these samples, spanning the 1st to 5th centuries AD, reveals sustained use of these local sedimentary resources throughout the Roman period.

Conversely, samples A09, A10 and A11 constitute a second group characterised by a coarser, darker brown ceramic matrix, less homogeneous and moderately optically active. Porosity is more pronounced and includes meso- to macro-scale planar voids, vesicles, and channels, indicative of a more open and less compact fabric. Temper content is lower (~10%), composed of a roughly equal mixture of granular and elongated particles with angular to sub-rounded morphologies. Grain size distribution is bimodal, ranging from coarse silt to coarse sand, with a predominance of angular grains and generally weak particle alignment and sorting.

Mineralogical assemblages in this group encompass quartz, potassium feldspar, plagioclase feldspar, muscovite—often exhibiting deformation textures—and opaque minerals. Lithic inclusions include quartzite, granitoid, and claystone fragments, suggesting a more complex source area. These textural and mineralogical differences indicate a distinct ceramic technology, likely reflecting alternative clay preparation methods and temper selection.

From a geological standpoint, the mineral and lithic inclusions in this second group point towards raw materials derived from the low-grade metamorphic rocks of the Ossa-Morena Zone, located east of the Jurassic sedimentary outcrops. This zone is characterised by Neoproterozoic to Palaeozoic metasedimentary formations such as meta-greywackes, meta-conglomerates, meta-cherts, meta-pelites, quartzites, and partially metamorphosed carbonates.

Table 2. Results of the study developed with OM. Mineral and rock fragments identification.*.

Lab ID	Mineralogy	Rock fragments	Observations
A01	Qz, K-Fsp, Pl, Ms.	Qzite.	Very abundant in Kfs (microcline) and Ms.
A02	Qz, K-Fsp, Pl, Ms.		Not homogenized Clp identified.
A03	Qz, K-Fsp, Pl, Ms.		Not homogenized Clp identified.
A05	Qz, K-Fsp, Pl, Am, Ms.		Rare Am. Not homogenized Clp identified.
A06	Qz, K-Fsp, Pl, Ms.		
A08	Qz, K-Fsp, Pl, Ms.		Not homogenized Clp identified.
A09	Qz, K-Fsp, Pl, Ms, Bt (very rare).	Qzite.	Ms-rich.
A10	Qz, K-Fsp, Pl, Ms, Bt (very rare).	Qzite, Clst, Gnrd.	Ms-rich.
A11	Qz, K-Fsp, Pl, Ms, Bt, Grt.	Qzite, Clst, Gnrd.	Ms- and Bt-rich.
A12	Qz, K-Fsp, Pl, Ms.		Not homogenized Clp identified.

* Abbreviations: Qz = Quartz, Kfs = Potassium-rich Feldspar, Pl = Plagioclase, Ms = Muscovite, Am = Amphibole, Bt = Biotite, Grt = Garnet, Qtzite = Quartzite, Clst = Claystone, Gnrd = Granitoid rock, Clp = Clay Pellets.

Table 3. Main characteristics of the ceramic matrix and the porosity *.

Lab Id	Ceramic paste				Porosity
	Color	Hom./Het.	Enrichment in Fe or Ca	Optical activity	Shape and size
A01	Brown	H.HOM.	Fe	S	Vesicles (meso)
A02	Red	H.HOM.	Fe	S	Vesicles (meso)
A03	Red	H.HOM.	Fe	S	Vesicles – Chanels (macro, mega)

 doi:10.20944/preprints202508.1919.v1

A05	Red	H.HOM.	Fe	S	Vesicles – Chanels (meso, macro)
A06	Red	H.HOM.	Fe	S	Vesicles (micro, macro)
A08	Red	H.HOM.	Fe	S	Vesicles (micro, meso)
A09	Brown	M.HOM.	Fe	S	Vesicles – Planar voids (meso, macro)
A10	Brown	M.HOM.	Fe	M	Vesicles – Chanels (meso, macro)
A11	Brown	M.HOM.	Fe	M	Vesicles – Chanels (meso, macro)
A12	Red	H.HOM.	Fe	NA	Vesicles (micro, meso)

* H.HOM., highly homogeneous; M.HOM., moderately homogeneous; S.HOM., slightly homogeneous; H.HET., highly heterogeneous; M.HET., moderately heterogeneous; S.HET., slightly heterogeneous. Fe, iron-rich matrix; S.Ca, slightly calcitic; M.Ca, moderately calcitic; H.Ca, highly calcitic. S, slightly optically active; M, moderately active; NA, not active.

Table 4. Main characteristics of the temper. *Main characteristics of the ceramic matrix and the porosity *.

LAB ID	Temper							
	Shape	Sphericity	Packing	Alignment	Sorting	GSD	DGSF	Temper %
A01	G	A-R	CS	P	M	U	VFS/FS	20
A02	G	A-R	CS	F	W	U	CSilt	10
A03	G	SR-R	CS	F	W	U	CSilt–VFS	20
A05	G	SR-R	CS	F	W	U	CSilt	20
A06	G	SA-R	CS	F	W	U	CSilt	10
A08	G	SR-R	CS	F	W	B	CSilt/CSand	10
A09	G/El	A-SR	CS	P	P	B	CSilt/CSand	10
A10	G/El	VA-SA	OS	P	P	U	FS	10
A11	G	A-SR	SP	M	M	B	VFS/CSand	10
A12	G	SA-R	CS	F	W	U	CSilt	20

* G, mainly granular grains; El, mainly elongated grains. VA, very angular; A, angular; SA, sub-angular; SR, sub-rounded; R, rounded; WR, well-rounded. CS, close spaced; SS, single spaced; DS, double spaced; OS, open spaced. P, weak alignment; M, moderate; F, strong. VP, very poor sorting; P, poor; M, moderate; W, well sorted. U, unimodal grain size distribution; B, bimodal. V, vesicles; Ch, channels; Pl, planar voids (mic = micro, mes = meso, mac = macro, meg = mega; e.g., V–Ch (mes/mac) = vesicles and channels, meso to macro scale). Grain size fractions: VFS, very fine sand; FS, fine sand; CSilt, coarse silt; CSand, coarse sand; VFS/FS, very fine to fine sand; CSilt–VFS, coarse silt to very fine sand; CSilt/CSand, coarse silt and coarse sand; VFS/CSand, very fine and coarse sand.

The mineralogical data obtained from powder XRD analysis (Table 5) reveal a broadly consistent firing regime across the assemblage, with quartz emerging as the dominant crystalline phase, accompanied by illite/muscovite, K-rich feldspars, plagioclase feldspars, hematite, biotite, and, in some cases, mullite. Sample A11 deviates slightly from this pattern, lacking mullite and instead comprising primarily quartz, illite/muscovite, K-rich feldspars, plagioclase feldspars, and biotite. While garnet was identified petrographically, its absence in the XRD spectra is likely attributable to its low abundance and detection limits inherent to the technique.

 doi:10.20944/preprints202508.1919.v1

Table 5. Mineralogical phases identified by powder XRD. *

Lab ID	Qz	Kfs	Pl	Hm	Cal	I/M	Bt	Mul
A02	xxxx	x	xx	x	vs	x		
A01	xxxx	xx		x		xx		
A03	xxxx	vs	vs	x		vs		
A05	xxxx	xx	vs	x		x		
A06	xxxx	xx	vs	x	vs	xx		
A08	xxxx	xx	vs	x		x		
A09	xxxx	xx	vs	vs		x		
A10	xxxx	x	vs	x		xxx		
A11	xxxx	xx	x	x		x	xxx	
A12	xxxx	xx		x				x

* xxxx = very abundant; xxx = abundant; xx = moderate; x = scarce; vs = traces.

The identification of temperature-sensitive mineral phases provides important insights into the thermal history of the ceramic assemblage [13–15]. The persistence of illite/muscovite, which decomposes at temperatures above 950 °C, indicates that most vessels were fired below this threshold. Hematite, typically forming at temperatures above 750 °C, was consistently detected, except in sample A12. These observations collectively suggest that the majority of the ceramics were fired within an estimated range of 750–950 °C.

Sample A12 is distinctive in its mineralogical profile, exhibiting the absence of illite/muscovite and the presence of mullite—a high-temperature neoformed phase that crystallises at firing temperatures exceeding 1000 °C [16]. This indicates that this vessel was subjected to significantly higher thermal conditions. Conversely, sample A11, which retains both illite/muscovite and hematite, likely experienced intermediate firing temperatures within the 750–950 °C range. Overall, these data point to a predominantly stable firing tradition with occasional technological variability, possibly reflecting differences in kiln design, fuel management, or functional requirements of specific vessel types.

XRF data provides further support for the differentiation in raw material selection. The two groups identified during optical microscopy analysis show distinctive SiO_2 vs Al_2O_3correlation, and Fe_2O_3/Al_2O_3 ratios (Figures 4A, 4B) indicating that phyllosilicates are importants mineralogicals phases to consider to differentiate ceramics as evidenced by OM and XRD. Trace element data, particularly Zr and Y concentrations (Figure 4C), provide additional diagnostic indicators. Samples A09, A10, and A11 exhibit distinct Zr/Y ratios, consistent with the presence of zircon minerals and implying the use of different tempering materials or clay sources for these vessels. These trace element signatures reinforce the separation of this group from the rest of the assemblage on both compositional and technological grounds.

 doi:10.20944/preprints202508.1919.v1

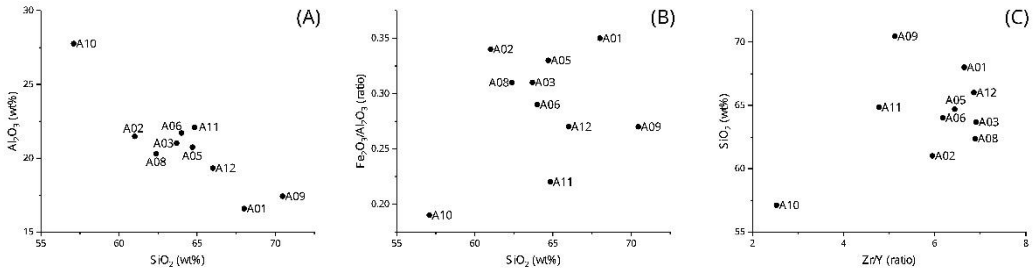

Figure 4. Binary plots of the analysed ceramic samples. A) CaO vs SiO_2; B) Fe_2O_3/Al_2O_3 vs SiO_2; C) SiO_2 vs Zr/Y. These diagrams illustrate compositional variability among the samples and are used to assess raw material sources and potential technological choices.

To further investigate the ceramic microstructure and inclusion characteristics, SEM-EDS analysis was conducted in tandem with the mineralogical and chemical approaches. Most samples exhibit a dense and homogeneous matrix, with porosity primarily represented by closed vesicles and isolated channels exhibiting low interconnectivity. In contrast, samples A09, A10, and A11 reveal markedly less compact fabrics, featuring frequent interconnected vugs, channels, and planar voids. These microstructural differences may reflect lower firing temperatures and/or shorter firing durations and are interpreted as indicative of distinct clay processing and firing protocols [17].

Elemental mapping reveals that silicon (Si), aluminium (Al), magnesium (Mg), and iron (Fe) are predominantly concentrated within the ceramic matrix, indicating their incorporation into the fine-grained clay fraction. In contrast, silicon (Si), potassium (K), and sodium (Na) are enriched in the temper grains, particularly within quartz, feldspars, plagioclases, and muscovite. Calcium (Ca) is generally associated with Na-rich plagioclase, but it is also frequently observed within the pore network, where it likely represents secondary calcite precipitated post-firing due to diagenetic processes. Titanium (Ti) occurs in discrete oxide mineral grains and is occasionally found in association with iron (Fe), suggesting the presence of ilmenite or similar accessory phases.

Of particular note are the large mica crystals—either muscovite or biotite—identified in samples A09, A10, and A11. These inclusions are chemically rich in K, Mg, and Fe and are distributed heterogeneously throughout the ceramic body (Figures 5 and 6). Their frequent occurrence further substantiates the geochemical and microstructural distinctiveness of this subgroup within the broader assemblage, reinforcing interpretations of divergent raw material sources and production techniques.

 doi:10.20944/preprints202508.1919.v1

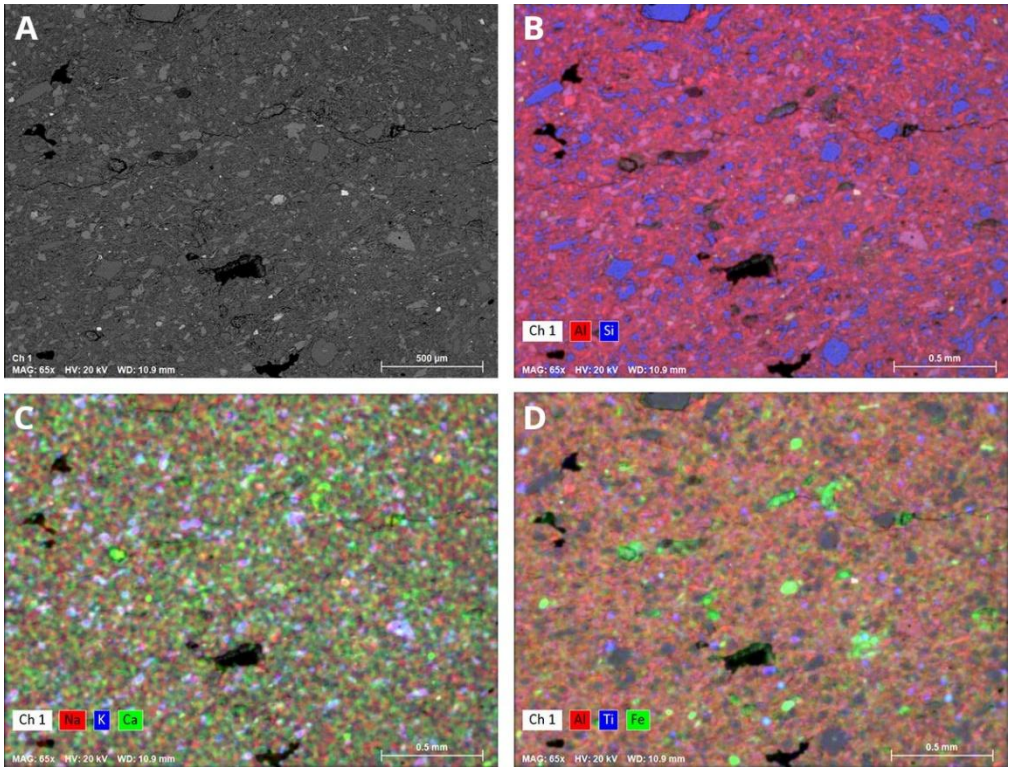

Figure 5. SEM/BSE image and chemical distribution maps of sample A06, showing the microstructural features of the ceramic matrix in backscattered electron (BSE) mode, accompanied by elemental maps highlighting the spatial distribution of key chemical components.

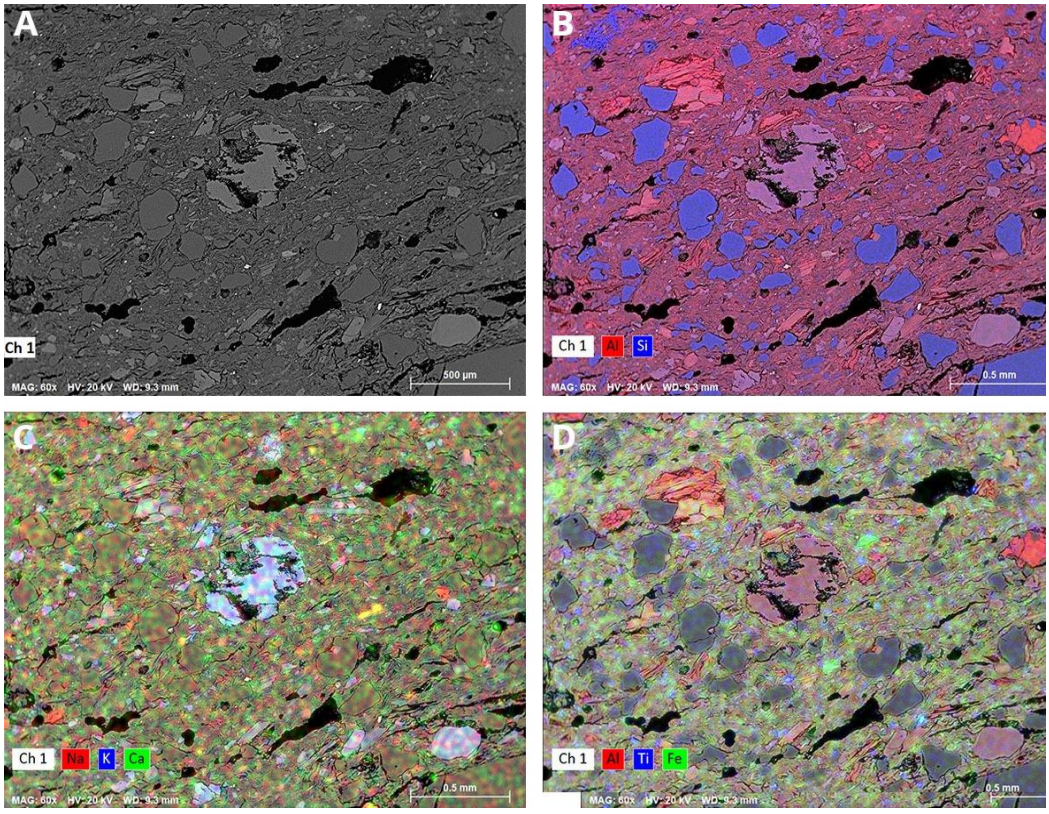

Figure 6. SEM/BSE image and chemical distribution maps of sample A11, showing the microstructural features of the ceramic matrix in backscattered electron (BSE) mode, accompanied by elemental maps highlighting the spatial distribution of key chemical components.

 doi:10.20944/preprints202508.1919.v1

To conclude, the mineralogical, geochemical, and microstructural data reveal significant variability in raw material selection, temper composition, and firing conditions—most notably in samples A09, A10, and A11. However, this variability does not correlate with either the chronological span of the assemblage or the typological classification of the vessels. These findings suggest a broad technological continuity across the period under study. The observed differences are thus more plausibly attributed to functional requirements or workshop-specific production strategies, rather than to temporal or morphological factors.

3.2. Amphora Functionality and Use: Evidence from Organic and Ceramic Data

Four of the amphorae discussed in the previous section—A08, A10, A11, and A12—were also analysed using Gas Chromatography–Mass Spectrometry (GC–MS) and Liquid Chromatography–Tandem Mass Spectrometry (LC–MS/MS), with the results recently published by Buraca et al. 2025 [18,19]. The primary aim of that study was not to explore the function or use of specific amphora types, but to evaluate the effectiveness of different analytical methods for identifying wine residues. These results are now incorporated into the present study to complement the ceramic fabric compositional analyses. The combination of molecular, chemical, and mineralogical data provides a more nuanced and substantiated interpretation of the vessels' functional roles, while also offering insights into how specific technological choices may have shaped their use within local economic and distributional contexts.

Sample A12 exhibited a similar molecular fingerprint, confirming the presence of Pinaceae-derived pitch, evidenced by dehydroabietic and 7-oxo-dehydroabietic acids, simonellite, retene, and the methylated forms of abietane-type acids. No wine-related biomarkers were detected in this sample, which instead showed a profile consistent with the storage of animal fats. The lipid spectrum included 1-monopalmitin, 1-monostearin (the most prominent peak), and lesser quantities of diacylglycerols such as 1,2-distearin and 1,3-distearin. Moreover, important peaks of undegraded triglycerides including triolein ($C_{57}H_{104}O_6$) and its analogues ($C_{55}H_{102}O_6$, $C_{55}H_{102}O_6$) were detected, suggesting minimal alteration or a more recent depositional context. The P/S ratio of 1.4 confirms a predominance of animal fats (Figure 7).

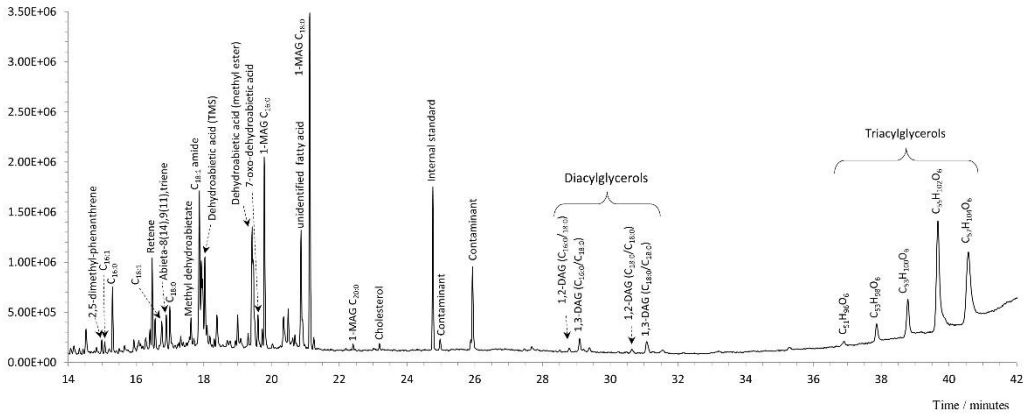

Figure 7. Chromatographic profile of sample A12.

Sample A08 lacked any detectable resinous coating or wine-associated compounds. Instead, presented a complex lipid signature marked by extensive degradation, with both monoacylglycerols and diacylglycerols identified. The P/S ratio, also calculated at 1.4, again points toward the presence of animal fats. Crucially, the identification of nitrogenous organic compounds such as hexadecanamide, octadecenamide, and octadecanamide suggested exposure to elevated temperatures, possibly related to the processing or cooking of animal products [20,21]. These amides are known to form via reactions between fatty acids and ammonia or amino groups under thermally intensive conditions, reinforcing the hypothesis of heat treatment or culinary use.

 doi:10.20944/preprints202508.1919.v1

Samples A10 and A11 revealed molecular signatures associated with biomass burning [22]. Both samples contained levoglucosan, a pyrolysis product of cellulose and hemicellulose, indicating exposure to burning plant matter. Additional markers such as pimaric acid and abietane-type diterpenoids (abietic, dehydroabietic, and 7-oxo-dehydroabietic acids) confirm the presence of aged pine resin. These results suggest that the amphorae contents may have been subjected to heating, potentially involving plant materials or seeds.

In summary, the residue analyses point to a diversified use of amphorae at Conimbriga. Some vessels were demonstrably coated with pine resin-derived pitch to ensure impermeability, consistent with the storage of liquids such as wine or oil. However, lipid residues in multiple samples indicate the presence of animal fats, suggesting the transportation or storage of semi-solid or solid organic products. The frequent occurrence of pitch in conjunction with lipids highlights the multifunctional use of these containers. Nonetheless, it should be acknowledged that the absence of certain biomarkers in some vessels may result from post-depositional degradation processes, rather than a definitive absence of those contents during antiquity.

4. Conclusions

This multidisciplinary investigation of the Conímbriga amphorae assemblage provides a nuanced understanding of the technological and functional dimensions of ceramic production and use in Roman Lusitania. By integrating petrographic, mineralogical, geochemical, microstructural, and organic residue data, the study elucidates the interplay among production traditions, raw material sourcing, firing regimes, and vessel functionality.

Two primary technological traditions emerge, distinguished by their distinct raw materials, temper characteristics, and firing conditions. The first tradition is defined by fine-grained, well-sorted temper derived from fluvially deposited sediments in the Mondego River basin. These ceramics display high compositional homogeneity and were fired under controlled conditions at moderate temperatures (ca. 750–950 °C), suggesting established workshop protocols and consistent access to local clay resources.

In contrast, the second tradition, exemplified by samples containing coarser, angular inclusions derived from the low-grade metamorphic rocks of the Ossa-Morena Zone, reflects a less refined paste preparation and possibly shorter or lower-temperature firing. This variation suggests the coexistence of alternative production strategies, perhaps associated with distinct workshops, functional requirements, or adaptations to resource availability.

Notably, these technological distinctions do not align with chronological phases or vessel typologies within the assemblage. This lack of correlation implies enduring technological continuity across time and form. Consequently, differences in raw material selection and processing likely reflect functional needs or workshop-specific traditions rather than shifts in ceramic types over time.

The integration of organic residue data reinforces this interpretation. Vessels associated with the fine-grained ceramic tradition—such as A08 and A12—frequently display traces of Pinaceae-derived pitch, indicating deliberate impermeabilisation, alongside lipid residues attributable to animal fats, and in at least one case potential wine biomarkers. This combination of features suggests these amphorae were tailored for liquid or semi-liquid contents requiring sealing. Conversely, samples with coarser paste and inclusions—namely A09, A10, and A11—lack resinous coatings and consistently display animal fat residues, indicating different functional uses that may not have necessitated waterproofing.

These correlations between technological tradition and vessel use are compelling, though they derive from a limited dataset. Thus, while indicative, they require cautious interpretation. Further research involving larger assemblages and broader contextual data will be essential for verifying and expanding upon these initial patterns.

Overall, this study demonstrates the complexity and diversity of ceramic production and use in Roman Conímbriga, highlighting how technological choices and functional imperatives intersected within local craft and economic systems. By adopting an integrative, multidisciplinary approach, the

 doi:10.20944/preprints202508.1919.v1

research advances our understanding of ancient production practices and paves the way for future studies that will further explore the relationships among technology, economy, and material culture in antiquity.

Author Contributions: Data curation: M.B.; Formal analysis I.B., C.O., M.B.; Funding acquisition I.B., V.H.C., J.M.; Investigation I.B., C.O., V.H.C., M.B.; Methodology C.O., M.B.; Project administration J.M., M.B.; Resources J.M.; Supervision V.H.C., J.M., M.B.; Validation C.O., J.M., M.B.; Writing - original draft I.B., C.O., C.B., V.H.C., N.S., M.B.; Writing - review & editing I.B., C.O., C.B., V.H.C., N.S., J.M. ,M.B. All authors have read and agreed to the published version of the manuscript.

Funding: The archaeometric study was funded by the Center of Cultural and Humanistic Studies of the University of Coimbra (CECH-UC) through the FCT project UIDB/00196/2019.

Data Availability Statement: The data presented in this study are available on request from the corresponding author.

Acknowledgments: Ida Buraca thanks the Foundation for Science and Technology (FCT) for funding her doctoral project, "Roman amphorae from the civitas of Conimbriga: supplying a civil center in Lusitânia," carried out in collaboration with the DGPC (FCT/DGPC-PRT/BD/152870/2021). César Oliveira acknowledges the Portuguese Science Foundation (FCT) for his Individual Scientific Employment contract (Doi: 10.54499/2020.00087.CEECIND/CP1593/CT0003). The authors also acknowledge the financial support of HERCULES Laboratory through projects UIDB/04449/2020 (Doi: 10.54499/UIDB/04449/2020) and UIDP/04449/2020 (Doi: 10.54499/UIDP/04449/2020), and IN2PAST Associate Laboratory through project LA/P/0132/2020 (Doi: 10.54499/LA/P/0132/2020), all funded by FCT and by the European Regional Development Fund.

Conflicts of Interest: The authors declare no conflicts of interest.

References

1. Correia, V.H., Conimbriga: a vida de uma cidade da Lusitânia. **2024**: Coimbra University Press.
2. Alarcão, J. and R. Etienne, Fouilles de Conimbriga: Alarcão, J., et al. Céramiques diverses et verres. Vol. 6. **1976**: Diffusion, E. de Boccard.
3. Alarcão, P., Construir na ruína: a propósito da cidade romanizada de Conimbriga. **2009**, Universidade do Porto (Portugal).
4. Reis, M.P., De Lvsitaniae Vrbium Balneis. Estudo sobre as termas e balneários das cidades da Lusitânia, 2 vols., Tese de doutoramento em Arqueologia. Coimbra: Universidade de Coimbra, **2014**.
5. Ruivo, J., V.H. Correia, and A. De Man, A cronologia da muralha baixo-imperial de Conímbriga. In Ruivo J. and V.H. Correia (eds.), Conimbriga diripitur. Aspetos das ocupações tardias de uma antiga cidade romana, Coimbra, Universidade de Coimbra, **2021**: p. 15-24.
6. Ruivo, J. and V.H. Correia, Conimbriga diripitur: aspetos das ocupações tardias de uma antiga cidade romana. Vol. 67. **2021**: Imprensa da Universidade de Coimbra/Coimbra University Press.
7. De Man, A. and A.M. Soares, A datação pelo radiocarbono de contextos pós-romanos de Conimbriga. Revista Portuguesa de Arqueologia, **2007**. 10(2): p. 285-294.
8. Alarcão, J., Fouilles de Conimbriga V, in La céramique commune locale et régionale, D. Boccard, Editor. **1975**: Paris.
9. Correia, V.H. and A. De Man, Variação e constância na ocupação de Conimbriga e do seu território. **2010**, CIDEHUS.
10. Correia, V.H., I. Buraca, R. Triães and C. Oliveira, Identificação de uma produção de ânforas romanas no norte da Lusitânia. Revista Portuguesa de Arqueologia, **2015**. 18: p. 225-136.
11. Quinn, P.S., Ceramic petrography: the interpretation of archaeological pottery & related artefacts in thin section. **2013**.
12. Wentworth, C.K., A Scale of Grade and Class Terms for Clastic Sediments. The Journal of Geology, **1922**. 30(5): p. 377-392.

 doi:10.20944/preprints202508.1919.v1

13. Riccardi, M., B. Messiga, and P. Duminuco, An approach to the dynamics of clay firing. Applied Clay Science, **1999**. 15(3-4): p. 393-409.
14. Gliozzo, E., Ceramic technology. How to reconstruct the firing process. Archaeological and Anthropological Sciences, **2020**. 12(11): p. 260.
15. Maritan, L., et al., Influence of firing conditions on ceramic products: experimental study on clay rich in organic matter. Applied Clay Science, **2006**. 31(1-2): p. 1-15.
16. Heimann, R.B. and M. Maggetti, The struggle between thermodynamics and kinetics: Phase evolution of ancient and historical ceramics. In Artioli, G. and R. Oberti (eds.) The Contribution of Mineralogy to Cultural Heritage. European Mineral Union and the Mineralogical Society of Great Britain & Ireland, **2019**. p. 233-281.
17. Xanthopoulou, V., I. Iliopoulos, and I. Liritzis, Mineralogical and Microstructure Analysis for Characterization and Provenance of Ceramic Artifacts from Late Helladic Kastrouli Settlement, Delphi (Central Greece). Geosciences, 2021. 11(1): p. 36.
18. Oliveira, C., I. Buraca, V.H. Correia and R. Trigães, Análises químicas de ânforas identificadas em Conímbriga. Al-madan, **2015**. 19: p. 175-176.
19. Buraca, I., C. Olveira, G. Elesi, J. Connan, R. Morais and V.H. Correia, In vino veritas. An assessment of current research of amphorae contents from Conimbriga (Portugal). DIAITA: Food&Heritage, **2025**. 2: e0207.
20. Lejay, M., et al., The organic signature of an experimental meat-cooking fireplace: The identification of nitrogen compounds and their archaeological potential. Organic Geochemistry, **2019**. 138: p. 103923.
21. 40. Lejay, M., et al., Organic signatures of fireplaces: Experimental references for archaeological interpretations. Organic Geochemistry, **2016**. 99: p. 67-77.
22. Correia, V. H., Burada, I., Triães, R., Araújo, A., & Oliveira, C. *Identification of a production of Roman amphorae in Northern Lusitania*. In C. Oliveira, R. Morais, & Á. M. Cerdán (Eds.), ArchaeoAnalytics - Chromatography and DNA analysis in archaeology (pp. 169-184). Esposende City Council. **2015**.